Epitaxial Crystal Growth of Nitratine on Calcite (10.4) Cleavage Faces at the Nanoscale

Raúl Benages-Vilau,*[,†] Teresa Calvet,[†] Miquel Angel Cuevas-Diarte,[†] Carlos Pimentel,[‡,§] and Carlos M. Pina[‡,§]

[†]Departament de Cristal·lografia, Mineralogia i Dipòsits Minerals, Facultat de Geologia, Universitat de Barcelona (UB), c/Martí i Franquès s/n, 08028 Barcelona, Spain

[‡]Departamento de Cristalografía y Mineralogía, Universidad Complutense de Madrid, E-28040 Madrid, Spain [§]

Instituto de Geociencias IGEO (UCM-CSIC), c/José Antonio Novais 2, E-28040 Madrid, Spain

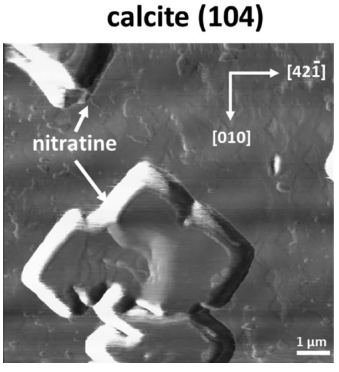

ABSTRACT: In this article, we present a study of the epitaxial growth of nitratine ($NaNO_3$) on calcite ($CaCO_3$) from ethanolic solutions. By using sodium nitrate saturated solutions in ethanol we were able to observe the initial stages of nitratine crystallization on calcite (10.4) cleaved surfaces with atomic force microscopy (AFM). Although the oriented epitaxial growth of nitratine crystallites on calcite is independent from the solvent used (water, ethanol, or mixtures of them), the use of ethanolic solutions saturated with respect to nitratine is preferable for surface imaging in the AFM fluid cell. Additional nanotribology AFM experiments allowed us to measure shear strengths necessary to remove crystallites of nitratine from calcite (10.4) faces. On the basis of both AFM observations and measured shear strengths, the mechanism of epitaxial growth of nitratine on calcite (10.4) is discussed.

1. INTRODUCTION

Epitaxial layers are of great interest in science and industry. They are important for the formation of corrosion coatings, the improvement of the quality of interfaces between metals and silicates, and also for producing coatings that provide specific chemical or abrasive properties to materials.[1] Furthermore, controlling the deposition of epitaxial layers is essential for the production of high-quality semiconductors and nanotechnol-ogical devices.[2,3]

In nature, epitaxial growth of mineral phases is also a very common phenomenon. Indeed, mineral epitaxies have been the first epitaxial systems studied systematically (e.g., epitaxies involving feldspars of sodium and potassium, quartz on orthoclase, rutile on hematite, and chalcopyrite on enargite).[4]

A fundamental parameter that controls epitaxial growth is the misfit between the surface lattice of overgrowth and substrate crystals. This misfit is usually quantified with the following simple expression:

$$\delta = \frac{L_{\text{sub}} - L_{\text{over}}}{L_{\text{over}}} \times 100 \qquad (1)$$

where L_{sub} and L_{over} are the surface lattice parameters of the substrate and the overgrowing crystal, respectively.

According to the classical Royer's law, epitaxial growth can be only observed when absolute lattice misfit values are lower than 15%. Furthermore, lattice misfits seem to inversely relate to the adhesion between overgrowths and substrate and, therefore, determine the epitaxial growth mechanisms, i.e., Frank−Van der Merwe, Volmer−Weber, and Stranski−Krastanov.[3] While a continuous layer-by-layer growth (Frank−Van der Merwe mode) is generally observed for low lattice misfits, the formation of oriented three-dimensional islands on a substrate (Volmer−Weber mode) occurs when the lattice misfits are relatively high. Only for intermediate lattice misfits the spreading of a number of continuous monolayers is followed by the formation of three-dimensional islands, as the Stranski −Krastanov epitaxial mode describes. Despite the scientific and technological importance of epitaxial growth, the thermodynamics, kinetics, and crystallographic controlling param-eters of this phenomenon remain little known. In this regard, the epitaxy of nitratine crystals on calcite (10.4) faces is an excellent model example to further investigate both the features and the controlling factors of epitaxial growth at ambient conditions.[2]

In the Landolt Bornstein database there are listed many examples where nitratine acts as a substrate for the epitaxial growth of different organic molecules (e.g., succinic acid and diacetyldioxym) and inorganic compounds (mainly alkaline halides). More interestingly, in the same database some examples where nitratine is the deposited material (e.g., on calcite, dolomite, and baritocalcite) are provided.[5]

Although the crystallization of nitratine on calcite is a well-known example of epitaxy since decades ago, it has not been deeply studied. Aspects such as the mechanism of epitaxial growth, the stability, and the adhesion of nitratine monolayers on the calcite (10.4) face still remain poorly understood.

According to Déo and Finch, nitratine can easily grow epitaxially on the {10.4} cleavage faces of calcite.[6] Certainly, this was the first recorded example of epitaxy.[7] While these authors found that the calcite substrate has little or no influence on the nitratine rate of growth, Barlow and Pope made the first detailed geometrical analysis of the epitaxial relationships in the $NaNO_3$– $CaCO_3$ system.[8] Complementary, Glikin and Plotkina studied the inverse process, i.e., how calcite microcrystal slurries adhere onto a growing nitratine seed.[9] These authors found that almost 40% of calcite crystals are epitaxially oriented, whereas the rest are not oriented but are joined by vertices or edges.

Nitratine and calcite crystallize at room temperature in the R3c space group with Z = 6. The cell parameters, considering a hexagonal lattice, are a_0 = 5.070 Å, c_0 = 16.82 Å for nitratine[10] and a_0 = 4.99 Å, c_0 = 17.06 Å for calcite.[11] These two minerals are a classical example of isoestructural compounds[2] because, even though they have an identical crystal structure, they do not form a continuous series of solid solutions.

In the epitaxy of nitratine on calcite, the [421] and [010] directions are parallel on the common (10.4) epitaxial face. According to previous descriptions (ref 11 and references therein), rectangular lattices with the following dimensions can be defined on the calcite and nitratine (10.4) surfaces: $a_{nitratine}$ = 0.811 nm and $b_{nitratine}$ = 0.507 nm for nitratine and $a_{calcite}$ = 0.810 nm and $b_{calcite}$ = 0.499 nm for calcite. From these parameters, lattice misfits calculated using eq 1 are −0.12% along the [421] direction and −1.58% along the [010] direction. These values are well below the general accepted misfits required for epitaxy to occur. Furthermore, because of such low lattice misfits, a strong adhesion between nitratine and calcite (10.4) faces can be expected.

The objective of the work presented in this article is to investigate the initial stages of nitratine epitaxial growth onto calcite (10.4) surfaces by optical microscopy, scanning electron microscopy (SEM), and atomic force microscopy (AFM). Of special interest to characterize the epitaxy of nitratine on calcite are both the nanoscale growth experiments conducted in the fluid cell of the AFM and the subsequent nanotribological study of the epitaxial overgrowths. This article is part of a general study on the relationships between structure, ionic charge, and crystal growth behavior of sodium nitrate, calcite, and other isostructural compounds.[12,13]

2. MATERIALS AND METHODS

2.1. Microscale Crystallization Experiments. A number of preliminary crystallization experiments were carried out to optimize the experimental conditions to subsequently study the epitaxial growth of nitratine on calcite (10.4) with AFM. For conducting such experiments, natural calcite, sodium nitrate, distilled water, and ethanol were used. Analytical grade $NaNO_3$ was supplied by Quality Chemicals.[14] Its purity was checked by ionic coupled plasma spectrometer with a mass detector (Perkin-Elmer Optima 3200 RL): we found 21.7 ppm of titanium and 0.22 ppm of manganese, and thus no more purification was carried out. X-ray diffraction pattern (Panalytical X'pert Pro diffractometer at room temperature with Bragg−Brentano geometry with a hybrid monochromator and a X'Celerator Detector) confirmed that the powder supplied by Quality Chemical was nitratine, i.e., the low temperature phase of sodium nitrate (II-$NaNO_3$). The samples used as substrates were calcite crystals of optical quality from Durango (México). Prior to each experiment, calcite crystals were cleaved in small pieces with a razor blade parallel to their {10.4} faces. Then drops of nitratine saturated solutions were deposited on the cleaved crystals and left to evaporate. Sodium nitrate crystallization was visualized with an optical microscope. The results of the crystallization were subsequently studied by SEM. Experiments with saturated solutions in water, in 25% water−75%ethanol mixtures, and in pure ethanol were carried out.

In the case of pure ethanolic solutions, a number of experiments were also conducted by immersing small pieces (about 5 × 5 × 2 mm) of cleaved calcite {10.4} rhombohedra during 30 min in stirred ethanolic solutions saturated with respect to nitratine. Three different calcite surfaces (10.4) were used as substrates: (i) freshly cleaved surfaces, (ii) cleaved surfaces washed for 30 min with deionized water, and (iii) surfaces washed for 1 min with diluted HCl and then for 40 min in deionized water.

After reaction of calcite surfaces with nitrate ethanol solutions, the crystals were removed and dried at 40 °C for 30 min.

Molecular simulations have shown that at room temperature there is a quick interchanging of water molecules between the adsorbed layer on calcite {10.4} faces and the solution bulk.[15] In contrast, an ethanol adsorbed layer is very difficult to desorb once formed. Even more, ethanol molecules can displace the adsorption layer of water.[15] In addition, dissolved $NaNO_3$ molecules surely capture some water molecules that enter in the hydration shell of ions, and therefore, less water molecules remain absorbed on calcite. Thus, a significant effect of the cleaving conditions on the subsequent epitaxial growth is not expected once calcite crystals are immersed in ethanolic solutions

Characterization of the epitaxial overgrowths was made using a magnifying glass, optical microscope, and SEM. Either a Nikon SMZ 1500 magnifying glass with ProgRess speed XT^{core} 3 CCD camera or a Nikon Eclipse LV100POL microscope with DXM 1200F digital camera were used. The optical study was conducted using the equipment at Department de Cristal·lografia, Mineralogia i Dipòsits Minerals of the Universitat de Barcelona.

A selected number of samples was observed at room temperature in a Hitachi S-4100 field-emission scanning electron microscope (FE-SEM), located in Centres Cientifics i Tecnològics of Universitat de Barcelona (CCiT-UB). The samples were mounted on a slide (12 mm diameter) with a conductive adhesive (Agar Scientific) and covered with a fine carbon layer (ca. 20 nm).

2.2. AFM Observations. In situ nanoscale observations of epitaxial growth of nitratine on calcite (10.4) surfaces were performed with an atomic force microscope (AFM, Nanoscope IIIa Multimode, Veeco Instruments) of the Centro Nacional de Microscopia Electrónica (CNME-ICTS) at the Universidad Complutense de Madrid. This AFM is equipped with a $\sim 15 \times 15\ \mu m^2$ scanner and a fluid cell, which allows one to operate in static and flowing liquids. AFM images were taken in contact mode while displaying the height, deflection, and friction signals. Silicon nitride tips supported by triangular cantilevers with nominal force constants ranging from 0.06 to 0.58 N/m were used (Bruker SNL-10). In order to both optimize the quality of the images and highlight different features of surface structure, several filters, as well as different values for the *z*-limit and the integral and proportional gains, were used. The following AFM observations were performed: (i) on previously grown epitaxial layers on calcite (10.4) faces (ex situ observations) and (ii) on calcite substrates on which epitaxial growth was promoted by injecting ethanolic solutions saturated with respect to $NaNO_3$ in the fluid cell of the AFM (in situ observations). More than 600 images were collected and subsequently analyzed using the software provided by Nanoscope (5.30r3sr3) and Nanotec (WSxM).[16]

2.3. Nanotribology Experiments. Nanotribology experiments were addressed to wear or remove nitratine islands epitaxially grown on calcite (10.4) surfaces. For this purpose, the applied loading (vertical) force between the AFM tip and the surfaces was progressively increased till nitratine islands were either eroded or removed. In these experiments, both loading and frictional (lateral) forces can be calculated from AFM recorded signals in volts. Loading force was calculated by the following formula:

$$F_N = Sk_N V_N \quad (2)$$

where S is the sensitivity of the AFM photodetector in nm/V, k_N is the normal spring constant of the cantilever, and V_N is the cantilever deflection set point in volts. In the case of island removal, minimum shear strengths required for the detachment events were estimated using the simple formula

$$\tau = F_L/A \quad (3)$$

where F_L is the lateral force and A is the area of contact between the removed nitratine island and the calcite (10.4) surface. In eq 3, lateral forces were calculated with the equation[17−19]

$$F_L = \frac{3h}{2L} k_T S V_L \quad (4)$$

where k_T is the torsional spring constant of the cantilever where the tip is supported, h is the height of the tip (including half of the cantilever thickness), L is the length of the cantilever, and V_L is half of the difference in voltage of the trace and retrace frictional signals. The torsional spring constant can be calculated using the relationship

$$k_T = \frac{Gwt^3}{3h^2 L} \quad (5)$$

where G is the shear modulus of the cantilever, and w and t are its width and thickness, respectively.

For the nanotribology experiments, tips supported by rectangular cantilevers (Bruker TESP) were used since their calibration is easier than for the case of triangular cantilevers. AFM images were processed with the Nanoscope (5.30r3sr3) and Nanotec (WSxM) softwares.[16]

3. RESULTS AND DISCUSSION

3.1. Epitaxy of Nitratine on Calcite from Aqueous and Ethanol Solutions. Cleaved calcite {10.4} rhombohedra become almost completely enclosed by nitratine crystals when they are immersed in saturated sodium nitrate aqueous solutions or water−ethanol solutions, which are led to evaporate to dryness (Figure 1). In all cases, relatively few but large nitratine crystals grew sharing the same orientation with respect to the calcite substrates, i.e., the growth is epitaxial.

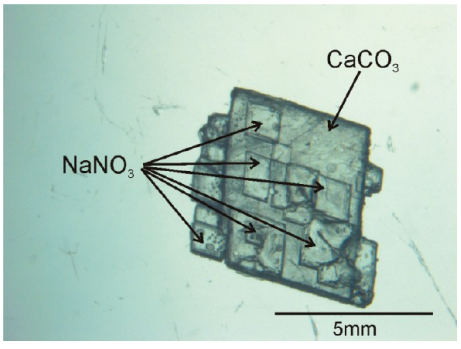

Figure 1. Single calcite crystal coated by an aggregate of nitratine crystals. The nitratine crystals formed by evaporation of an aqueous solution initially saturated with respect to $NaNO_3$.

Differently, when pure ethanol saturated in sodium nitrate was used, the formation of a higher amount of nitratine crystallites on calcite cleavage surface occurs. Crystallites obtained from pure ethanolic solutions are smaller than those grown from water and water−ethanol solutions, and they do not cover completely the calcite surfaces. Figure 2 shows a calcite cleavage surface with a large number of nitratine crystallites deposited on it. These samples were obtained after the immersion of calcite crystals in saturated $NaNO_3$ ethanolic solution for 30 min. Nitratine crystallites are all similar in size, with a low degree of coalescence and highly oriented with respect to the calcite (10.4) substrate. Frequently, nitratine crystallites are joined together to form large chains of crystals, which decorate macro- and microsteps produced during the cleaving process of calcite substrates.

A comparison of Figures 1 and 2 clearly shows that epitaxial growth of nitratine on calcite from ethanolic solutions results in a higher nucleation density and more homogeneous crystal size distribution compared to the epitaxial growth from aqueous solutions initially saturated with respect to nitratine. This is due to the fact that the solubility of $NaNO_3$ in ethanol is much lower than that on water. As a consequence, nucleation at higher supersaturations is expected when ethanol is used as a solvent. This makes the use of ethanol more suitable than water to conduct epitaxial growth experiments in the fluid cell of an AFM.

3.2. Nanoscale Observations and Nanotribology Study of Epitaxial Overgrowths. After verifying that nitratine crystals formed from ethanol solutions are epitaxially deposited on calcite (10.4) cleavage surfaces, we investigated the epitaxial growth phenomenon at the nanoscale using AFM. For this purpose we have performed (i) ex situ AFM observations of the epitaxial crystals previously grown in the laboratory, (ii) in situ nanoscale growth experiments consisting in the promotion of epitaxial growth of nitratine on calcite (10.4) substrates in the fluid cell of the AFM, and (iii) nanotribology experiments that allowed us to obtain information about the stability and adhesion of the epitaxial overgrowths.

3.2.1. Ex Situ AFM Observations. First AFM observations were made after the epitaxial growth of nitratine occurred onto both freshly cleaved calcite surfaces and calcite surfaces previously washed with water. Although because of slight dissolution calcite substrates washed with water (with and without previous treatment with HCl) are rougher than freshly cleavage calcite surfaces, epitaxial growth of nitratine was observed in both cases.

In all the samples studied, epitaxial nitratine overgrowths do not coat completely calcite substrates. Moreover, nitratine islands reach a thickness of tens to hundreds of nanometers without significant coalescence. Figure 3 shows an example of water washed calcite surface in contact with an initially saturated $NaNO_3$ ethanolic solution for 30 min. Considering that the solution became supersaturated with respect to nitratine, this kind of deposit indicates that we can exclude the Frank−van der Merwe epitaxial mechanism (perfect wetting), and the choice is limited between the Stranski−Krastanov and the Volmer− Weber growth mechanisms. Moreover, taking into account that the major part of substrate is free from nitratine nucleation, the Volmer−Weber mechanism seems to be the most effective one.

High-resolution AFM images of both the calcite (10.4) substrate and the nitratine overgrown crystals further demon-strate that the growth is epitaxial with an almost perfect coincidence of crystallographic directions. Figure 4A,B shows high-resolution images of both calcite and nitratine (10.4) surfaces. As can be seen in these figures, nitratine and calcite rectangular surface lattices are parallel and practically indis-tinguishable from each other.

Surface lattice parameters determined from fast-Fourier transform (FFT) maps constructed from a selected number of high-resolution AFM images are $a_{nitratine} = 8.8 \pm 0.4$ Å and $b_{nitratine} = 5.3 \pm 0.3$ Å for nitratine and $a_{calcite} = 9.0 \pm 0.1$ Å and $b_{calcite} = 5.2 \pm 0.3$ Å for calcite. These calculated parameters are in good agreement with surface lattice parameters as obtained from nitratine and calcite bulk structures. Therefore, significant surface reconstruction of the nitratine lattice can be discarded.

3.2.2. In Situ Nanoscale Growth Experiments. Figure 5 shows the initial stages of epitaxial growth of nitratine on a freshly cleaved calcite (10.4) surface. A few minutes after injecting an ethanolic solution saturated with respect to nitratine in the fluid cell of the AFM, nitratine nuclei start to form on the calcite surface. Nucleation preferentially occurs on the calcite step edges, and only a

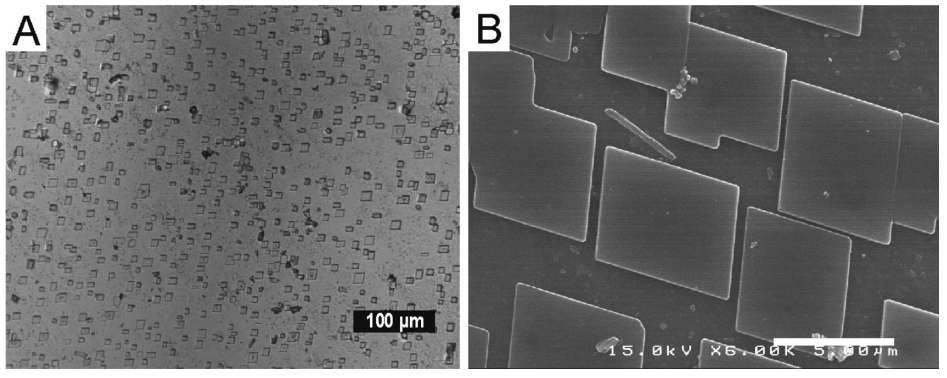

Figure 2. Epitaxial crystallization from an ethanolic solution of $NaNO_3$ onto calcite (10.4) faces. (A) Image taken with an optical microscope. (B) SEM image. Both samples were in contact with a saturated $NaNO_3$ ethanolic solution for 30 min.

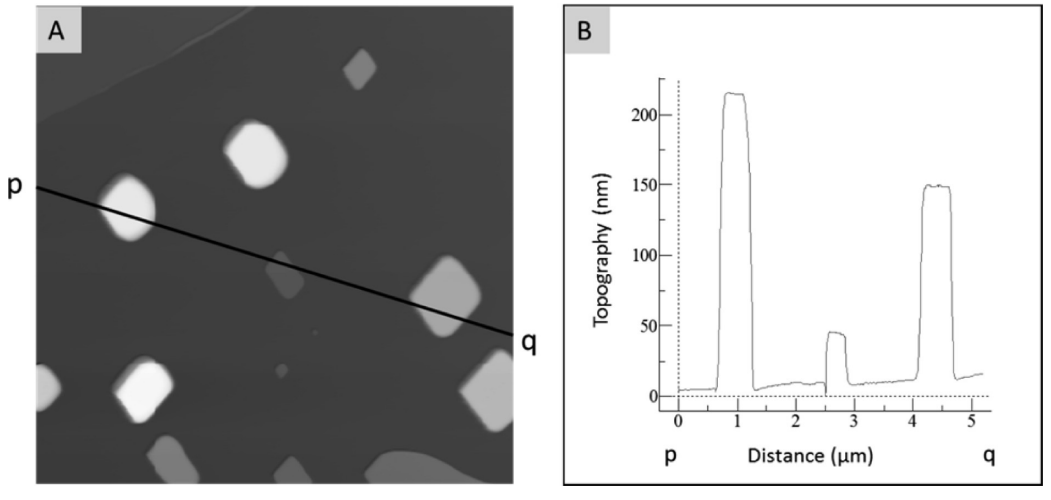

Figure 3. (A) AFM topography image of nitratine rhombohedra grown over a water washed (10.4) calcite surface. Scan area: 5 × 5 μm^2. (B) Profile along the line p−q marked in panel A. The sample was in contact with a saturated ethanolic solution for 30 min.

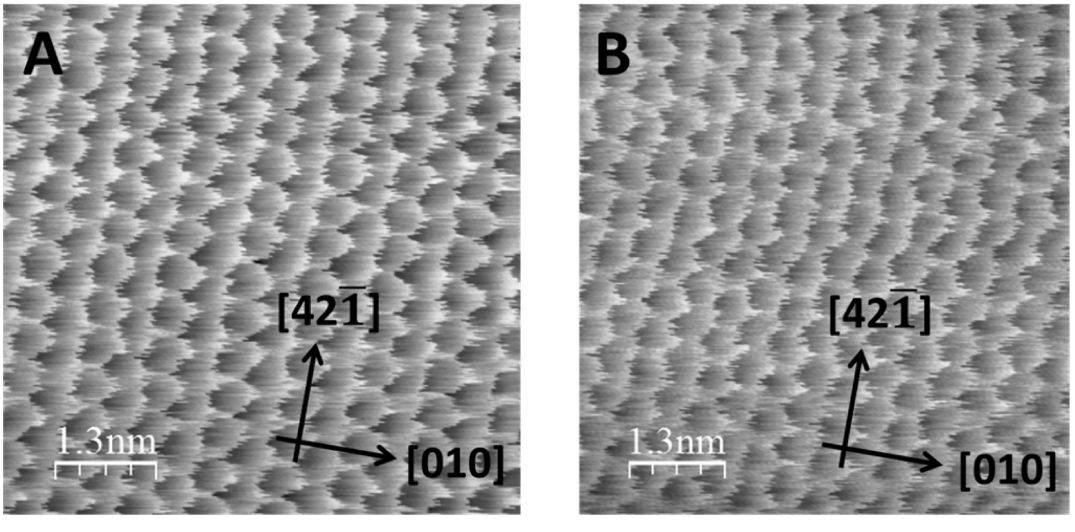

Figure 4. High-resolution AFM friction images of nitratine grown on calcite (10.4). (A) Surface lattice of the calcite (10.4) substrate. Scan area: 6 × 6 n m ^{2}.(B) Surface lattice of the nitratine (10.4) plane epitaxially grown on the calcite substrate. Scan area: 6 × 6 n m ^{2}.

few nuclei form on the calcite terraces. Since calcite samples are cleaved manually, surface features and defects are necessarily different from one sample to another. Therefore, the calcite coverage by nitratine is different for different observed surfaces.

While nitratine nuclei on the terraces tend to dissolve with time, nuclei formed on the step edges grow. This is a nice example of the re-entrant angle effect generated by the geometry of the steps (3D nuclei form even if the bulk of the solution is

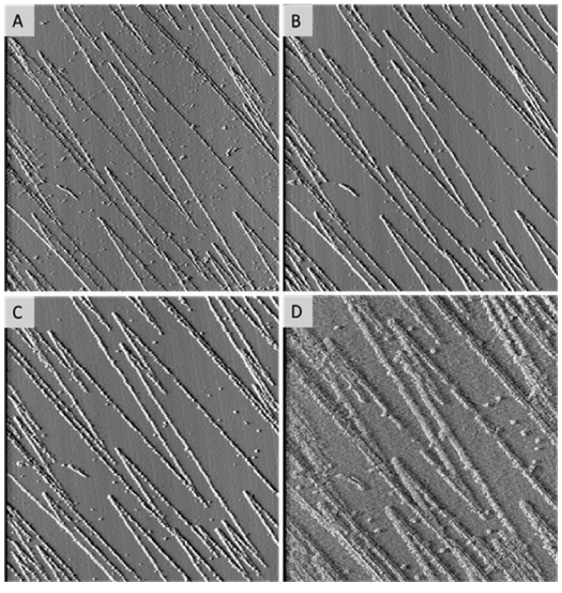

Figure 5. Sequence of AFM deflection images showing the early stages of the epitaxial growth nitratine crystallites onto a calcite (10.4) cleavage surface from a saturated ethanolic solution. Crystals preferably nucleate onto cleavage edges. Scan area: 5 × 5 μm^2. Time of the sequence: 2 h and 18 min.

close to equilibrium).[20] This slightly depletes the solution bulk supersaturation, and hence, most nuclei on terraces vanish.

In a few minutes, the height of the islands ranges from ∼0.3 nm to ∼1.5 nm, i.e., one to five nitratine monolayers (∼0.3 nm in height). As crystallization proceeds, nitratine islands accumulate along the steps edges, their lateral spreading being limited, i.e., repeated two-dimensional nucleation is faster than the layer-by-layer covering of the substrate. This behavior indicates again a Volmer−Weber epitaxial growth mechanism.

When comparing Figures 2 and 5, we can observe that even though the reaction time in the former case is about 4 times less, the resulting nitratine crystals are larger than those grown in the cell of the AFM. Such a difference is mainly due to the difference in the volume and conditions of the growth solutions. While crystals shown in Figure 2 grew from 20 mL of a $NaNO_3$ ethanolic solution under continuous stirring, crystals shown in Figure 5 grew from a stagnant $NaNO_3$ ethanolic solution confined in a volume of about 50 μL.

3.2.3. Nanotribology Experiments. The tip of the AFM was used to wear or remove nitratine islands epitaxially grown on calcite substrates. These nanotribology experiments were conducted in a liquid environment (i.e., ethanolic solutions) to minimize capillarity forces. These experiments allowed us to obtain information about the adhesion between nitratine overgrowths and calcite (10.4) faces.

Typically, large nitratine islands (i.e., islands with areas of about 5 × 5 μm^2 and heights larger than 300 nm) are easily eroded by the tip of the AFM when loading forces are increased (see Figure 6). When loading forces are high enough ($F_N \approx 80$ μN), nitratine islands become pyramidal after a few scans and their shape is the negative of the shape of the AFM tip. If the wearing process continues, islands vanish, and only a shadow of a few monolayers of nitratine remains on the calcite substrate. During the wear of large nitratine islands, calcite substrates are not damaged by the tip of the AFM. This is not surprising since nitratine is about 1 order of magnitude softer than calcite

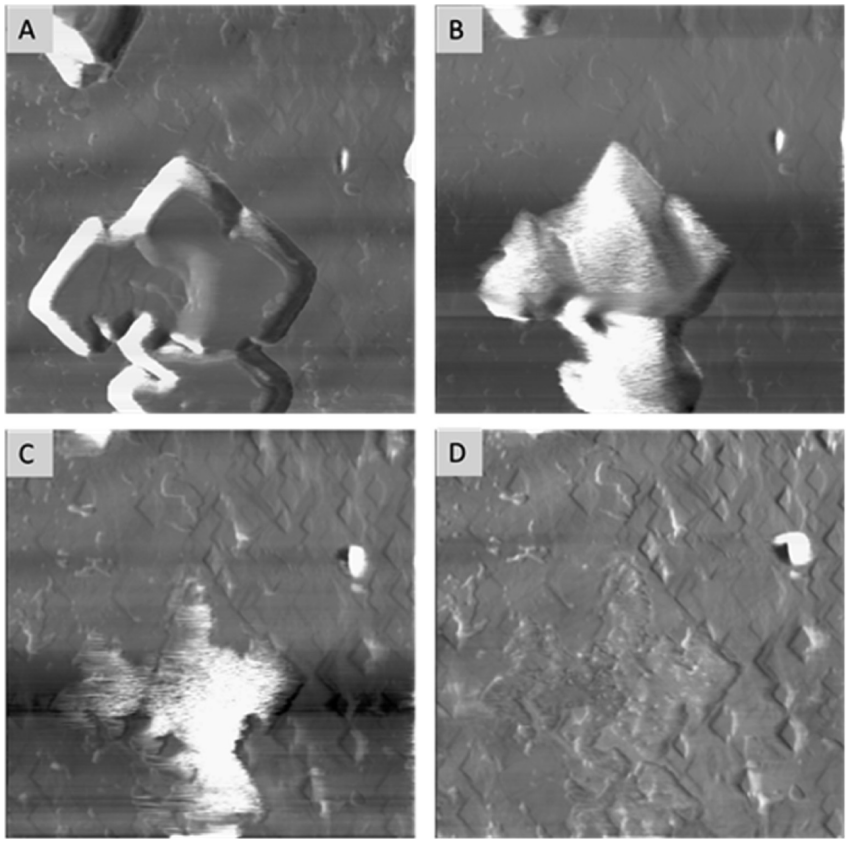

Figure 6. Sequence of AFM friction images showing the wearing of nitratine islands grown on a calcite (10.4) face. Scan area: 10 × 10 μm^2.

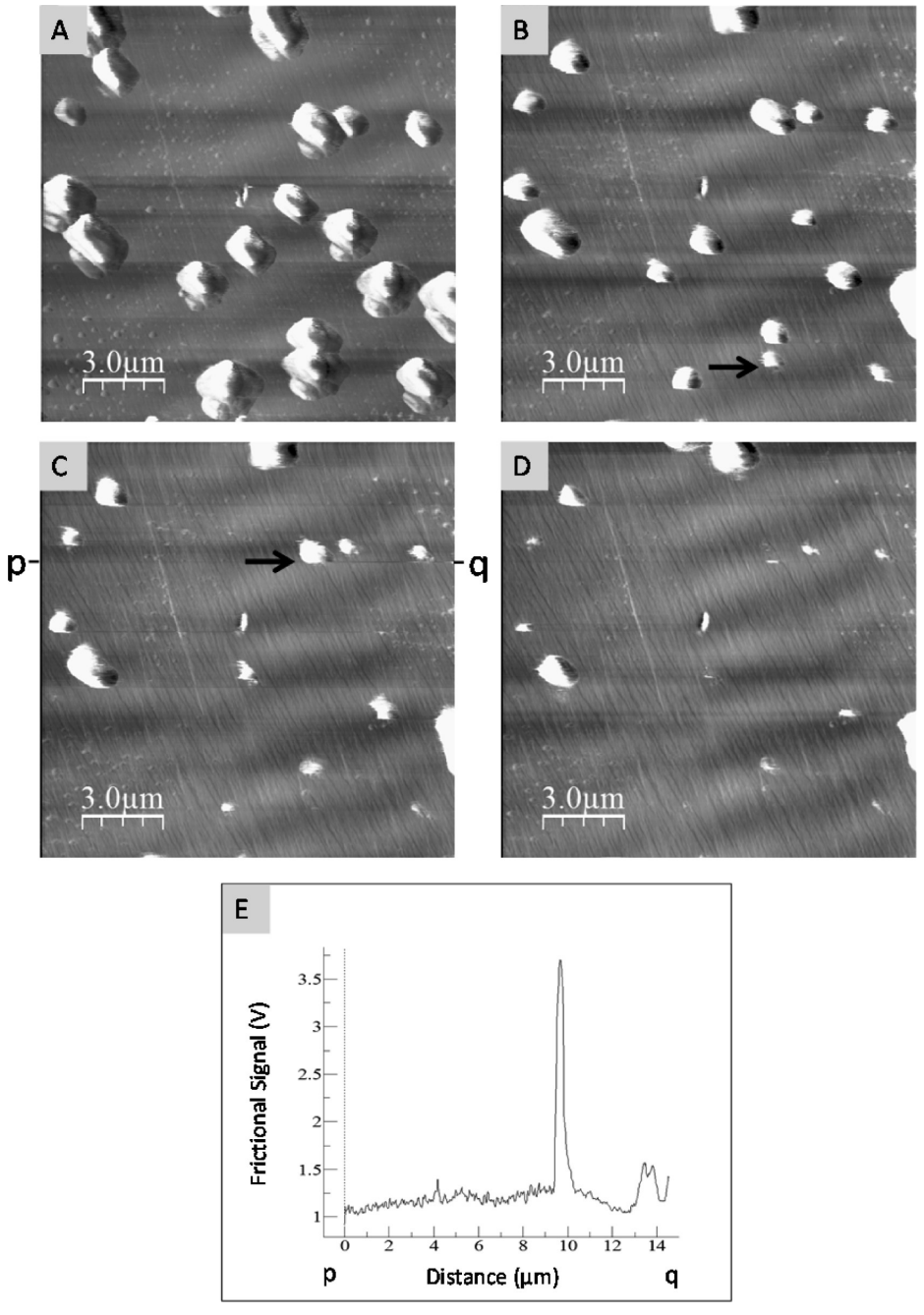

Figure 7. Detachment of nitratine islands grown on a calcite (10.4) surface. (A) Area of interest imaged with low normal force (F_N = 0.71 μN). (B) Nanomanipulation of one island marked with a black arrow (F_N = 7.90 μN). (C) Nanomanipulation of another island also marked with a black arrow (F_N = 15.09 μN). (D) Area of interest after the nanomanipulation. (E) Profile of the frictional signal taken along p−q in panel C. The main peak marks the detachment of a single nitratine island.

(Mohs hardness of 1.5−2.0 for nitratine compared to 3.0 for calcite), and at room temperature, its plastic behavior occurs at lower stresses than for calcite.[21]

When nitratine islands are small and isolated (with areas of about 1 × 1 μm^2 and heights ranging from 200 to 400 nm in height), their detachment from the calcite substrate occurs before significant wearing can be observed. Figure 7 shows friction AFM images for increasing loading forces of the same area where a number of nitratine islands grew. As can be seen in this figure, the progressive increase of the vertical force made by the tip of the AFM eventually results in the removal of nitratine islands (see Figure 7B,C). Once islands are removed they were not found again on the calcite surface, indicating that they were not dragged over the calcite substrate but lost in the ethanolic solution.

Detachment events are accompanied by peaks in the lateral friction force signal. From friction peaks and estimated contact areas of nitratine islands on calcite substrate, shear strengths can be calculated using eqs 3 and 4. We found that nitratine islands were usually detached from the calcite (10.4) surface for shear strengths $\tau \approx 30$ MPa. Previous experiments conducted on calcite islands epitaxially grown on dolomite and kutnahorite (10.4) surfaces provided shear strengths to remove such islands $\tau \approx 7$ MPa on dolomite and $\tau \approx 130$ MPa on kutnahorite.[17] These shear strengths were found to inversely relate to the

absolute misfit values between calcite and dolomite and kutnahorite structures projected on the (10.4) epitaxial plane ($\delta = -4.79\%$ for calcite on dolomite and $\delta = -3.17\%$ for calcite on kutnahorite, both along the [421] directions). Considering that for the epitaxial growth of nitratine on calcite (10.4) face the maximum misfit is $\delta = -1.58\%$ (along the [010] direction), a shear strength for island detachment higher than $\tau \approx 30$ MPa might be expected. Such a low shear strength can be due to a relative weakness of the bonds formed between the nitratine and calcite structures along the (10.4) contact plane. In the case of the epitaxy of calcite on dolomite or kutnahorite, crystal structures and charges of the CO_3^{2-} groups and cations (Ca^{2+}, Mg^{2+}, and Mn^{2+}) of the overgrowth and substrate compounds are essentially identical. In such a situation, it is reasonable that the adhesion between overgrowth and substrates is mainly controlled by the lattice misfits. In contrast, in the nitratine structure the constituent ions have lower net charges (i.e., Na^+ and NO_3^-), and a weaker adhesion of this compound on calcite (10.4) face is expected. A relatively low adhesion between nitratine and calcite (10.4) face would also explain the functioning of a Volmer−Weber epitaxial mode, despite the low lattice misfits between both structures.

4. CONCLUDING REMARKS

Epitaxial growth of nitratine on calcite (10.4) can be easily promoted by evaporation of aqueous and ethanolic solutions saturated with respect to $NaNO_3$. We found that, when pure ethanolic solutions are used, the number of nitratine crystals increase but that their sizes become smaller. This fact makes easier the study of the nitratine epitaxial growth using AFM. Nanoscale observations confirmed that the epitaxial growth occurs by the nucleation and coalescence of nitratine islands on calcite (10.4) faces. The analysis of atomic scale images of both nitratine islands and calcite surface demonstrates that over-growth and substrate lattices are perfectly parallel on the epitaxial (10.4) plane. AFM observations of the nitratine islands also showed that repeated nucleation along calcite step edges and on previously deposited nitratine layers are energetically favored compared to nucleation and spreading on calcite terraces. This clearly indicates the functioning of a Volmer−Weber epitaxial growth mechanism, which is characteristic for low adhesions between overgrowths and substrates. A low adhesion between nitratine and calcite (10.4) face is consistent with the relatively low shear strength, $\tau \approx 30$ MPa, required to detach nitratine islands from calcite faces in our nanomanulation AFM experiments. However, compared with the epitaxy of calcite on dolomite and kutnahorite, this shear strength value is unexpectedly low considering the low lattice misfit between nitratine and calcite structures. Therefore, our results indicate that epitaxial growth mechanisms depend not only on the misfits between structures involved but also on the nature and strength of the bonds formed in the epitaxial contact planes. The AFM study presented here have also shown that nanomanipulation is a new interesting way to quantitatively characterize epitaxial growth phenomena in liquid environments. Nevertheless, future systematic nanotribology experiments and computer modeling are still required to gain a better understanding of the parameters that control epitaxial growth both in nature and in industrial processes.

Notes

The authors declare no competing financial interest.

ACKNOWLEDGMENTS

This work was partially supported by the Spanish Government (Project MAT2012-24487 and MAT2011-27225), the General-itat de Catalunya through the Grup Consolidat (2009SGR1307), Xarxa de Referència R+D+I en Materiales Avançats per l'Energia (XaRMAE), and the Ministerio de Educacion through La Factoría de Cristalizacion (Consolider-Ingenio CSD2006-15). R.B.-V. acknowledges Abengoa enterprise for the financial support through a Cenit program Consorcio Solar de I+D ConSOLi+da. C.P. acknowledges financial support from the Spanish Government (FPU grant). The AFM study was carried out at ICTS Centro Nacional de Microscopia Electronica, (UCM) Madrid. Centres Cientifics i Tecnologics of Universitat de Barcelona (CCiT-UB) provided access to the SEM. We would like to thank Enrico Gnecco for critical reading of this article.

REFERENCES

(1) Gebhardt, M. Epitaxy. In *Crystal Growth: An Introduction*; Hartman, P., Ed.; North-Holland: Amsterdam, The Netherlands, 1973; pp 105−142.

(2) Herman, M. A.; Herman, M. A.; Richter, W.; Sitter, H. *Epitaxy: Physical Principles and Technical Implementation*; Springer: Berlin, Germany, 2004.

(3) Kern, R.; Le, L.; Metois, J. J. Basic Mechanisms in the Early Stages of Epitaxy. In *Current Topics in Material Science*; Kaldis, E., Ed.; North Holland: Amsterdam, The Netherlands, 1979; Vol. 3, pp 131−419.

(4) Sunagawa, I. *Crystal Growth, Morphology and Perfection*; Cambridge University Press: Cambridge, U.K., 2005.

(5) Epitaxies of Inorganic Deposit Crystals on Inorganic Substrate Crystals. http://www.springermaterials.com/docs/navigation.do?m=l_1_246793_2012.

(6) Déo, A. R.; Finch, G. I.; Ghapurey, M. K. *Proc. R. Soc. A* **1956**, *236*, 7−9.

(7) Wakkernagel, H. K. *Arch. Ges. Nat.* **1825**, *5*, 293.

(8) Barlow, W.; Pope, W. *J. Chem. Soc.* **1908**, *93*, 1528−1560.

(9) Glikin, A.; Plotkina, J. *Mater. Struct.* **1999**, *6* (2), 155−158.

(10) Paul, G. L.; Pryor, A. W. *Acta Crystallogr., Sect. B: Struct. Crystallogr. Cryst. Chem.* **1972**, *28* (15), 2700−2702.

(11) Rahe, P.; Schütte, J.; Kühnle, A. *J. Phys: Condens. Matter* **2012**, *084006*, 14.

(12) Massaro, F. R.; Bruno, M.; Aquilano, D. *Cryst. Growth Des.* **2010**, *7*, 2870−2878.

(13) Benages-Vilau, R.; Calvet, T.; Cuevas-Diarte, M. A.; Aquilano, D. In preparation.

(14) Quality Chemicals. http://www.qualitychemicals.com/cas/index.html.

(15) Cooke, D. J.; Gray, R. J.; Sand, K. K.; Stipp, S. L. S.; Elliott, J. A. *Langmuir* **2010**, *18*, 14520−14529.

(16) Horcas, I.; Fernandez, R.; Gomez-Rodriguez, J. M.; Colchero, J.; Gomez-Herrero, J.; Baro, A. M. *Rev. Sci. Instrum.* **2007**, *1*, 013705.

(17) Pimentel, C.; Pina, C. M.; Gnecco, E. *J. Cryst. Growth* **2013**, *13* (6), 2557−2563.

(18) Luthi, R.; Meyer, E.; Haefke, H.; Howald, L.; Gutmannsbauer, W.; Guggisberg, M.; Bammerlin, M.; Guntherodt, H. J. *Science* **1994**, *5193*, 1979−1981.

(19) Luthi, R.; Meyer, E.; Haefke, H.; Howald, L.; Gutmannsbauer, W.; Guggisberg, M.; Bammerlin, M.; Guntherodt, H. J. *Surf. Sci.* **1995**, *1*−3, 247−260.

(20) Boistelle, R.; Aquilano, D. *Acta Crystallogr., Sect. A: Cryst. Phys., Diffr., Theor. Gen. Crystallogr.* **1978**, *34*, 406−413.

(21) Handbook of Mineralogy. http://www.handbookofmineralogy.org.